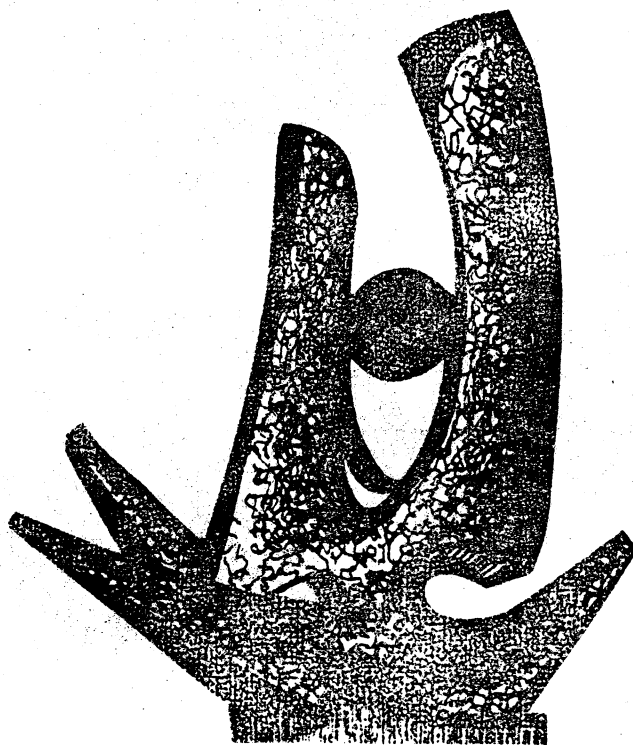


MICHIGAN STATE UNIVERSITY

CYCLOTRON LABORATORY

TRENDS OF LIGHT PARTICLE SPECTRA OBSERVED IN  
NUCLEUS-NUCLEUS COLLISIONS

T.C. AWES, G. POGGI, S. SAINI, C.K. GELBKE,  
R. LEGRAIN, and G.D. WESTFALL



JUNE 1981



Trends of light particle spectra observed in  
nucleus-nucleus collisions

T.C. Aves, G. Poggi,<sup>+</sup> S. Saini,<sup>++</sup> and C.K. Gelbke<sup>+++</sup>

Cyclotron Laboratory, Michigan State University  
East Lansing, Michigan 48824 USA

and

R. Legrain<sup>#</sup> and G.D. Westfall

Lawrence Berkeley Laboratory, Berkeley, California 94720 USA

<sup>+</sup> On leave from University of Florence, Italy

<sup>++</sup> On leave from Bhabha Atomic Research Center, India

<sup>+++</sup> Alfred P. Sloan Fellow

<sup>#</sup> On leave from C.E.N. Saclay, France

The emission of energetic light particles (p,d,t) has been studied for  $^{16}\text{O}$  induced reactions on Al, Zr and Au targets at the incident energies of 140, 215 and 310 MeV. The light particle energy spectra have been analyzed in terms of a moving thermal source. The apparent temperatures exhibit a systematic variation as a function of the incident energy per nucleon above the Coulomb barrier. The observed trend can be extrapolated in a smooth fashion to temperatures obtained in relativistic heavy ion collisions.

Information about the early stages of heavy-ion induced reactions may be obtained from the detection of energetic light particles which cannot be associated with evaporation from the compound nucleus.<sup>1-5</sup> At low energies (E/As20 MeV), recent experiments<sup>4-10</sup> have mainly used coincidence techniques to study detailed aspects of the reaction mechanisms producing energetic light particles. However, few single particle inclusive measurements have been published in this energy domain<sup>1,11,12</sup> and little information is available about the dependence of non-compound light particle emission on projectile, target and beam energy. In this communication, we report some of the results obtained from a survey of  $^{16}\text{O}$  induced reactions on Al, Zr, and Au targets at 140, 215, and 310 MeV beam energy.

The experiment was performed at the 88" cyclotron of the Lawrence Berkeley Laboratory using  $^{16}\text{O}$  beams of 140, 215 and 310 MeV incident energies. The following targets were used:  $^{27}\text{Al}$  (1.6 mg/cm $^2$  at 140, 215 and 310 MeV);  $^{90}\text{Zr}$  (20.9 mg/cm $^2$  at 215 and 310 MeV); and  $^{197}\text{Au}$  (1.2 mg/cm $^2$  at 140 MeV, 10.6 mg/cm $^2$  at 215 and 310 MeV). The thin Au target used at 140 MeV contained a hydrogen contaminant whose contribution to the proton spectra at forward angles has been removed in the analysis. Protons, deuterons and tritons were detected with two  $\Delta E-E$  telescopes each of 22 msr solid angle. The telescopes consisted of a 400  $\mu\text{m}$  thick surface barrier detector and a 7.6 cm thick NaI(Tl) detector which had a thin Havar window of about 75  $\mu\text{m}$  thickness. The energy calibration was established by measuring the elastic scattering of  $p + ^{197}\text{Au}$  at the beam energies of 10, 20, and 45 MeV. The resulting calibration was found to be linear over this energy region. It was extrapolated towards higher energies and used for all three hydrogen isotopes. The gain stability of the NaI(Tl) detectors was monitored by recording the  $\gamma$ -ray spectra of  $^{60}\text{Co}$  during ion source changes. The overall accuracy of the energy calibration is estimated to be about 3%. The absolute magnitude of the cross sections is accurate to within 35%.

As an example of the general features of the energy spectra that were observed in the present experiment, Fig. 1 shows the results for the  $^{197}\text{Au}(^{16}\text{O},p)$  reaction for three incident energies. The energy spectra are smooth structureless distributions which, at forward angles, extend to about

four times the incident energy per nucleon. With increasing detection angle, the cross sections decrease and the slopes of the energy spectra become steeper. Although these features are qualitatively similar to the ones reported in ref. 12, there is a difference in slope for the data at 310 MeV. (The reason for this discrepancy is not understood; however, we could reproduce our spectra at 310 MeV in two independently calibrated experiments.)

The cross sections can be rather well described in terms of a Maxwellian distribution observed in a rest frame that moves with a velocity intermediate between target and projectile,<sup>12-14</sup> see solid curves in Fig. 1. Correcting for the Coulomb repulsion from the target nucleus one obtains non-relativistically<sup>13,14</sup>

$$\frac{d^2\sigma}{dE d\Omega} = N_0(E-E_c)^k \exp\left(-\frac{(E-E_c)^k + E_1 - 2E_1^k(E-E_c)^k \cos\theta}{T}\right) \quad (1)$$

Here,  $E_c$  is the kinetic energy gained by the Coulomb repulsion from the target,  $E_1 = \frac{1}{2}mv^2$  is the kinetic energy of a particle at rest in the moving frame,  $T$  is the temperature and  $N_0$  is a normalization constant. The successful application of this parameterization should not be interpreted as evidence for a hot gas of nucleons separated from the target nucleus.<sup>13,14</sup> Rather, it indicates the randomization of light particle velocities in a rest frame that is different from the compound nucleus rest frame. In the present analysis, the values of  $E_c=0$ , 5 and 10 MeV were used for the Al, Zr and Au targets, respectively. The

best-fit source velocities lie in rather shallow  $\chi^2$ -minima and were found to be sensitive to the angular range over which the experimental cross sections were considered. In most cases, these velocities were found to be slightly less than half the relative velocity at grazing distance. The temperature parameter is, in general, rather well defined by the data and is less sensitive to the angular range considered. Variations of this parameter by 5% from the optimum values, resulted in typical increases of the  $\chi^2$ -values of 10%. A more detailed discussion will be given in a forthcoming paper. Here, we report on the systematic trends that were observed for the temperature parameter.

The temperature parameters determined in this experiment are shown in Fig. 2, where they are plotted as a function of  $(E-V_c)/A$ , the beam energy per nucleon above the Coulomb barrier. The Coulomb barrier in the laboratory was calculated according to  $V_c = (A_p + A_T)^{1/3} Z_p Z_T e^2 / A_p r_0 (A_p^{1/3} + A_T^{1/3})$ , where  $A_p, A_T$  and  $Z_p, Z_T$  are the mass and atomic numbers of projectile and target and  $r_0 = 1.44$  fm. For a given type of light particle, the apparent temperatures are approximately proportional to  $((E-V_c)/A)^{1/2}$  or, equivalently, proportional to the relative velocity of projectile and target at the point of contact (see insert of Fig. 2). Such a dependence is not expected from compound nucleus emission. It rather suggests more rapid processes such as knock-out or, perhaps, the formation of a thermalized subset of nucleons consisting of about equal numbers of target and projectile nucleons. The deduced

values of  $T$  are systematically larger for deuterons and tritons than for protons. At present, it is not clear whether this effect could be due to different contributions to the spectra from more equilibrated processes such as compound nucleus evaporation.

The parameterization used to describe our data is similar to the thermal models<sup>15,16</sup> that have been used to describe light particle spectra from relativistic heavy-ion collisions. In order to compare the trends observed at low energies to the ones at relativistic energies, we have determined the temperature parameters for the reaction  $^{20}\text{Ne} + \text{NaF} + p$  at energies of  $E/A = 400$  and  $800$  MeV<sup>17</sup> by using the relativistic generalization of eq. (1):

$$\frac{E d^2 \sigma}{p^2 dp d\Omega} = N_0 \gamma(E - \beta c \cos \theta) \exp(-\gamma(E - \beta c \cos \theta)/T) \quad (2)$$

where  $\beta$  is the velocity of the source ( $c=1$ ),  $\gamma = (1-\beta^2)^{-1/2}$  and  $E = (p^2 + m^2)^{1/2}$ . In order to minimize the contribution from projectile fragmentation and knock-out<sup>17</sup> we have restricted the data to large transverse momenta ( $\theta \geq 45^\circ$ ) for the determination of  $T$ . Despite the simplicity of the parameterization, the fits are of acceptable quality (see Fig. 3). The resulting temperature parameters are included in Fig. 2.

As is obvious from Fig. 2, the trends observed at low energies can be connected in a smooth fashion to the observations at high energies. For orientation, the solid and dashed curves have been calculated for relativistic Fermi and Boltzmann gases consisting of equal nucleon contributions

from target and projectile. In this case, the excitation energy per nucleon,  $\epsilon^*$ , is related to the incident kinetic energy per nucleon above the coulomb barrier,  $(E-V_C)/A$ , by

$$\epsilon^* = (m_0^2 + \frac{1}{2}m_0(E-V_C)/A)^{\frac{1}{2}} - m_0 \quad (3)$$

where  $m_0$  is the nucleon rest mass.

The excitation energy per nucleon of the gas is given

by

$$\epsilon^* = \langle \epsilon(T) \rangle - \langle \epsilon(T=0) \rangle \quad (4)$$

where  $\langle \epsilon(T) \rangle$ , the average kinetic energy per nucleon at temperature  $T$ , is obtained from the following relations:

$$\langle \epsilon(T) \rangle = \frac{V}{N} \frac{g}{2\pi^2 h^3} \int_0^\infty \epsilon(p) f(p, T) p^2 dp \quad (5)$$

$$N/V = \frac{g}{2\pi^2 h^3} \int_0^\infty f(p, T) p^2 dp \quad (6)$$

with the distribution function given by

$$f(p, T) = \frac{1}{\alpha \exp[(\epsilon(p) - \mu(T))/T]} \quad (7)$$

Here  $g$  is the spin-isospin degeneracy factor,  $\epsilon(p) = (p^2 + m_0^2)^{\frac{1}{2}} - m_0$  is the kinetic energy of the nucleon, and the chemical potential  $\mu(T)$  is determined from eq. (6) assuming normal nuclear density,  $N/V = 0.17 \text{ fm}^{-3}$ . For the Boltzmann gas one has  $\alpha=0$ ,  $\langle \epsilon(T=0) \rangle = 0$ ; and for the Fermi gas one has  $\alpha=1$  and  $\langle \epsilon(T=0) \rangle = 3/5 \epsilon_F$ , where  $\epsilon_F$  is the Fermi energy.

The general trend of the experimental temperature parameters is seen to follow the one depicted by the Fermi gas curve. Although the observed trends suggest the thermaliza-

tion of a subset of nucleons it should also be investigated whether alternative approaches such as single or multiple nucleon scattering models or hydrodynamical models would predict similar trends.

In summary, the inclusive light particle spectra of the present study may be parameterized in terms of a single thermal source that moves with slightly less than half the beam velocity. The extracted temperature parameters exhibit a systematic variation with the incident energy per nucleon at grazing distance. This variation can be extrapolated towards the temperatures extracted for relativistic nucleus-nucleus collisions. At present, it is not understood why the temperature parameters extracted for protons, deuterons and tritons are different at low energies. More experimental information will be necessary to investigate whether the observed trends persist for different target-projectile combinations and at intermediate energies.

This material is based upon work supported by the National Science Foundation under Grant No. PHY 78-22696 and in part by the Office of Basic Energy Sciences, Division of Nuclear Sciences, U.S. Department of Energy.

## References

1. H.C. Britt and A.R. Quinton, Phys. Rev. 124 (1961) 877.
2. D.H.E. Gross and J. Wilczyński, Phys. Lett. 67B (1977) 1.
3. J.P. Bondorf, J.N. De, A.O.T. Karvinen, G. Fai, and B. Jakobsson, Phys. Lett. 84B (1979) 162.
4. R.K. Bhowmik, E.C. Pollacco, N.E. Sanderson, J.B.A. England, and G.C. Morrison, Phys. Rev. Lett. 43 (1979) 619.
5. T.C. Aves, C.K. Gelbke, B.B. Back, A.C. Mignerey, K.L. Wolf, P. Dyer, H. Breuer, and V.E. Viola, Jr., Phys. Lett. 87B (1979) 43.
6. M. Bini, C.K. Gelbke, D.K. Scott, T.J.M. Symons, P. Doll, D.L. Hendrie, J.L. Lavielle, J. Mahoney, M.C. Mermaz, C. Olmer, K. van Bibber, and H.H. Wieman, Phys. Rev. C22 (1980) 1945, and refs. given therein.
7. H. Yamada, D.R. Zolnowski, S.E. Cala, A.C. Kahler, J. Pierce, and T.T. Sugihara, Phys. Rev. Lett. 43 (1979) 605.
8. K. Siwek-Wilczyńska, E.H. du Marchie van Voorthuysen, J. van Popta, R.H. Siemssen, and J. Wilczyński, Phys. Rev. Lett. 42 (1979) 1599.
9. J.H. Barker, J.R. Beene, M.L. Halbert, D.C. Hensley, M. Jääskeläinen, D.G. Sarantites, and R. Woodward, Phys. Rev. Lett. 45 (1980) 424.
10. R.P. Schmitt, G.J. Wozniak, G.U. Rattazzi, G.J. Mathews, R. Regimbart, and L.G. Moretto, Phys. Rev. Lett. 46 (1981) 522.
11. J.B. Ball, C.B. Fulmer, M.L. Mallory, and R.L. Robinson, Phys. Rev. Lett. 40 (1978) 1698.
12. T.J.M. Symons, P. Doll, M. Bini, D.L. Hendrie, J. Mahoney, G. Mantzouranis, D.K. Scott, K. van Bibber, Y.P. Vijogi, H.H. Wieman, and C.K. Gelbke, Phys. Lett. 94B (1980) 131.
13. T.C. Aves, C.K. Gelbke, G. Poggi, B.B. Back, B. Glagola, H. Breuer, V.E. Viola, Jr., and T.J.M. Symons, Phys. Rev. Lett. 45 (1980) 513.
14. T.C. Aves, G. Poggi, C.K. Gelbke, B.B. Back, B. Glagola, H. Breuer, and V.E. Viola, to be published in Phys. Rev. C.
15. G.D. Westfall, J. Gosset, P.J. Johansen, A.M. Poskanzer, W.G. Meyer, H.H. Gutbrod, A. Sandoval, and R. Stock, Phys. Rev. Lett. 37 (1976) 1202.
16. J. Gosset, J.I. Kapusta, and G.D. Westfall, Phys. Rev. C18 (1978) 844.
17. S. Nagamiya, M.C. Lemaire, E. Moeller, S. Schnetzer, G. Shapiro, H. Steiner, and I. Tanihata, Lawrence Berkeley Laboratory Report LBL-12123, to be published, and private communication.

## Figure Captions

FIG. 1. Energy spectra of protons detected in the reaction  $^{197}\text{Au}(^{16}\text{O},\text{p})$  at incident energies of 140, 215, and 310 MeV. The curves have been calculated with eq. (1) of the text.

FIG. 2. Temperature parameters for the proton, deuteron, and triton spectra in  $^{16}\text{O}$  induced reactions on targets of Al, Zr, and Au at incident energies of 140, 215, and 310 MeV and for the reaction  $\text{Ne} + \text{NaF} + \text{p}$  at 400 and 800 MeV/A. The solid and dashed curves are explained in the text.

FIG. 3. Spectra of protons detected in the reaction  $\text{Ne} + \text{NaF} + \text{p}$  at 400 and 800 MeV/A incident energies (from ref. 17). The curves have been calculated using eq. (2) of the text.



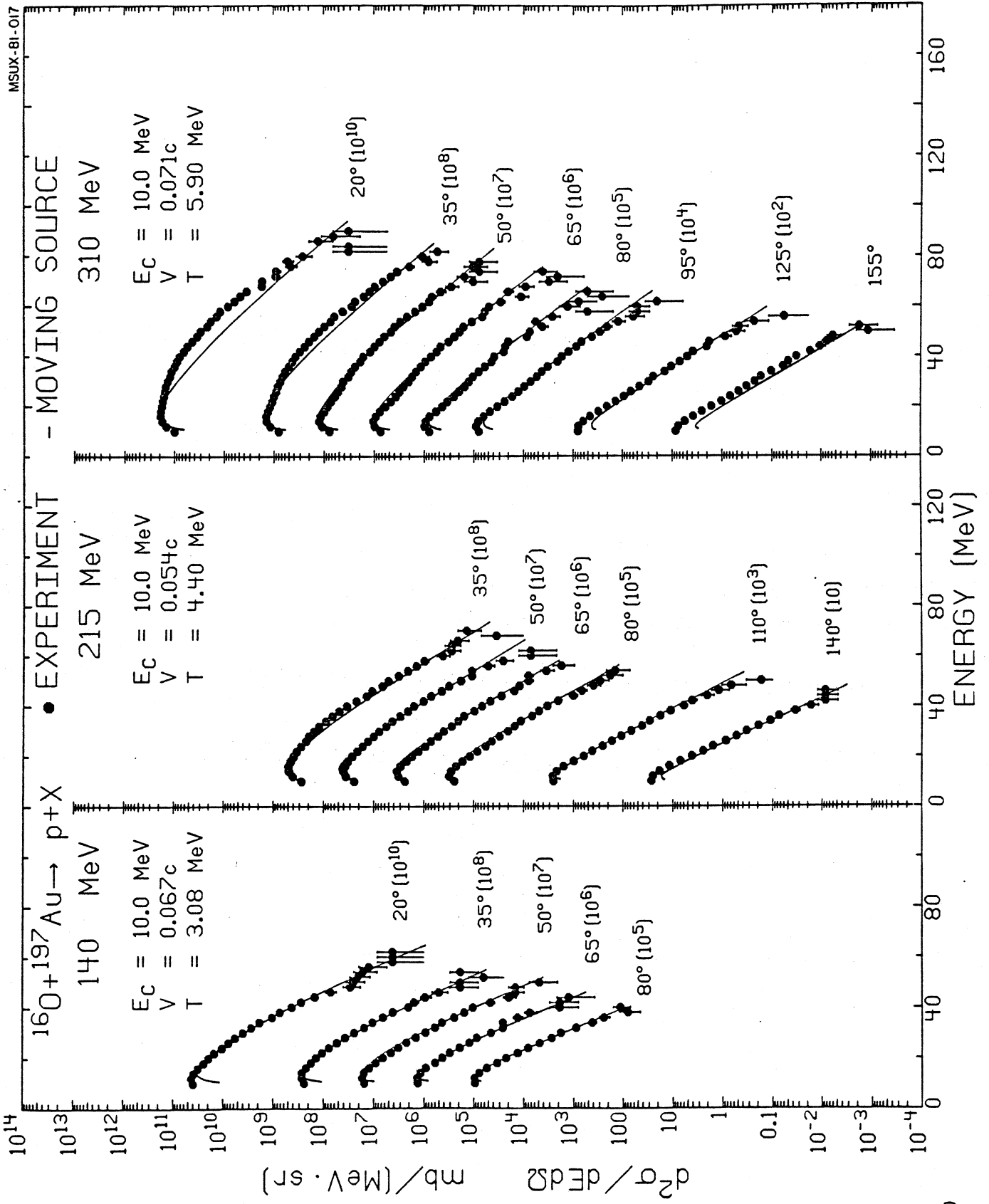


Fig. 1

Fig. 1

